SAC0307-*x*Ni/Ni 焊点的 IMC 及镍镀层的消耗

王玲玲，　孙凤莲，　王丽凤，　赵智力
（哈尔滨理工大学 材料学院，哈尔滨　150040）

摘　要：利用扫描电镜（SEM）对焊点 SAC0307/Ni（Sn-0.3Ag-0.7Cu/Ni）和 SAC0307-0.05Ni/Ni（Sn-0.3Ag-0.7Cu-0.05Ni/Ni）经过 180 ℃老化后的界面金属间化合物（IMC）的微观结构及镍镀层的消耗进行了研究. 结果表明，回流焊后，SAC0307/Ni 和 SAC0307-0.05Ni/Ni 焊点的 IMC 层均为 $(Cu_{1-x}Ni_x)_6Sn_5$，且随着老化时间的延长，IMC 层的厚度均逐渐增加，化合物类型没有变化，但 IMC 的化学组成有所改变. SAC0307-0.05Ni/Ni 焊点中 IMC 层形貌为蠕虫状，厚度比不加镍时有所降低. 回流焊后两种钎料焊盘的镍层消耗几乎相同，但老化 384 h 后 SAC0307/Ni 的焊盘镍层的剩余厚度明显比 SAC0307-0.05Ni/Ni 的小. 因此，钎料中添加适量的镍可以有效地降低焊盘镍层在时效过程中的消耗速率，即显著提高镍焊盘的抗老化能力.

关键词：SAC0307-*x*Ni；钎料；镍盘；金属间化合物；老化
中图分类号：TG425.1　　文献标识码：A　　文章编号：0253－360X(2009)11－0053－04

王玲玲

0　序　　言

在实际的电子封装中，由于镍具有明显的阻挡锡向基板中扩散生成过厚的金属间化合物的作用而常用作基板镀层，所以在 SnAgCu/Cu 之间引入镍阻挡层，能改善焊点的可靠性，具有较好的应用前景[1]. 但在长期的服役条件下，由于老化引起的焊盘镍层的消耗也是一个值得关注的问题. 因此研究镍焊盘对焊点性能的影响具有一定的实际意义.

除焊接基板因素外，焊料的选择对焊点可靠性也有影响. 研究表明，适量的 IMC 可以起到提高接头强度、润湿焊料及阻碍焊料扩散及氧化的作用. 然而数量过多，IMC 层过厚或者分布不均，在服役过程中会导致严重的应力集中、焊点抗剪强度的下降、焊点断裂韧性和抗低周疲劳能力下降，最终危害接头的性能而造成封装破坏[2－4]. Sn-Ag-Cu 合金体系因其具有相对较好的钎焊工艺性能和焊点可靠性，已逐渐被公认为最有应用前景的合金体系，通过改变合金中各成分的配比或者添加微量元素改善钎料的性能是目前国内外研究较多的课题[5,6]. 目前在 SnAgCu 钎料合金的基础上添加第四种元素已显示出良好的效果[7]. Sn-Ag-Cu 合金中加入镍可以改善润湿性和强度，微量的镍可以细化焊料合金的微观组织，从而提高焊料的综合力学性能. 文中采用镍作为扩散阻挡层，研究并讨论了 SAC0307 钎料中加入 0.05%Ni（质量分数）后对回流焊后及时效后的焊点界面 IMC 扩散行为及镍焊盘镀层消耗的影响.

收稿日期：2009－06－02
基金项目：国家自然科学基金资助项目（50575060）；哈尔滨市科技创新人才研究专项资金资助项目（RC2006QN006012）

1　试验方法

试验按 Sn-0.3Ag-0.7Cu-*x*Ni（x＝0，0.05）的质量配比，选用原料为纯度大于 99.9%的锡粒、银丝、铜丝以及 Sn-10Ni 中间合金，采用 ZRY55 真空加热炉熔炼制备出 SAC0307 及 SAC0307-0.05Ni 钎料合金. 试验用镍焊盘选择加工表面光滑且镀镍的纯铜板作为基板焊盘（直径为 2 mm），厚度约为 7 μm，用无水乙醇清洗干净后备用，助焊剂为松香溶液.

将 SAC0307 及 SAC0307-0.05Ni 焊料分别放在镍盘上，滴加数滴助焊剂后在回流焊机中进行焊接. 回流焊的峰值温度为 250 ℃，焊接时间为 500 s，最后在回流炉中风扇冷却，分别得到了 SAC0307/Ni，SAC0307-0.05Ni/Ni 焊点. 将制备的焊点进行等温老化试验，在 180 ℃下分别保温 0，24，96，216，384 h 后取出. 将回流焊后和老化后的焊点用环氧树脂镶嵌，经过粗磨、细磨、粗抛光、精抛光后制备成金相试样. 为了便于对 IMC 形貌的观察分析，金相试样用体积分数为 92% CH_3CH_2OH＋5% HNO_3＋3% HCl

的腐蚀液腐蚀 15 s，腐蚀好的试样表面喷一薄层金以便于SEM 观察及分析界面 IMC 形貌.

2 试验结果与分析

2.1 SAC0307-*x*Ni/Ni 焊点的 IMC

图 1 为 SAC0307/Ni 和 SAC0307-0.05Ni/Ni 回流焊后的界面 IMC 形貌. 由图 1 可知，经 250 ℃回流焊后，钎料与镍焊盘之间形成了化合物，化合物形貌均为比较均匀的细小针状，EDX 结果显示图 1a，b 中化合物均为$(Cu_{1-x}Ni_x)_6Sn_5$，但两种钎料形成的 IMC 化学组成有所不同，即$(Cu_{1-x}Ni_x)_6Sn_5$ 中的 Cu 和 Ni 原子的比例有所不同. 焊料中的银并没有参加与镍的反应. 此生成化合物类型的试验结果与 Lin 的理论相一致. 根据 Lin 等利用相图解释的含铜钎料和镍焊盘之间生成 IMC 层的形成机制，从 240 ℃的 Sn-Cu-Ni 三元相图的等温截面图可知，铜在纯锡中的溶解度大约为 1.1%. 当在纯锡中加入少量的镍时，铜的溶解度下降到大约 0.6%. 当铜的含量大于 0.6%时，趋向于生成化合物$(Cu_{1-x}Ni_x)_6Sn_5$ 相.

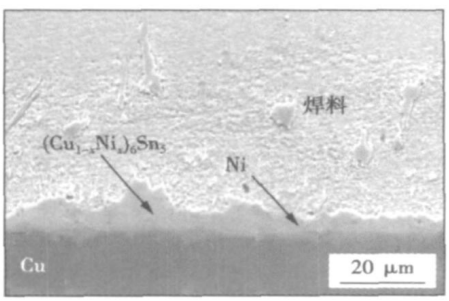

(a) SAC0307/Ni

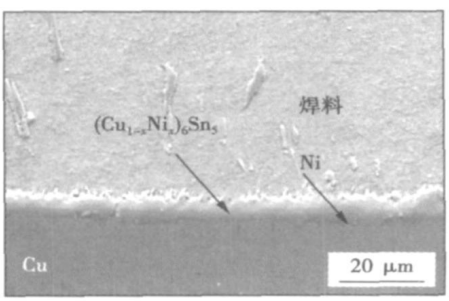

(b) SAC0307-0.05Ni/Ni

图 1 回流焊后界面 IMC 的形貌

Fig. 1 Morphology of IMC after reflow

图 2 为 SAC0307/Ni 和 SAC0307-0.05Ni/Ni 在 180 ℃下老化 384 h 后的界面 IMC 形貌. 从图 2 中可知，随着老化时间的增加，界面 IMC 的厚度均有所增加，但 SAC0307-0.05Ni/Ni 焊点的 IMC 厚度增长缓慢，明显比 SAC0307/Ni 的厚度降低. EDX 结果显示图 2a，b 中老化后的 IMC 成分仍均为$(Cu_{1-x}Ni_x)_6Sn_5$，这表明其为初始生成的 IMC，这是由于焊料中 Cu 元素含量为 0.7%，与 Lin 的相图解释相符. 图 2a 的 IMC 形貌老化后趋于平坦，图 2b 的 IMC 形貌为蠕虫状，在不致密的 IMC 内部有钎料夹杂. 焊盘 Ni 原子的扩散渠道是通过$(Cu_{1-x}Ni_x)_6Sn_5$ 向钎料中固态扩散，这是一个缓慢的动力学过程，高温老化促进了界面化合物两侧元素的扩散速率，形成了更多的界面化合物$(Cu_{1-x}Ni_x)_6Sn_5$. 镍在锡基钎料中溶解度较小，Sn-Ni 金属间化合物扩散速率比较低，对铜的消耗有扩散阻挡的作用.

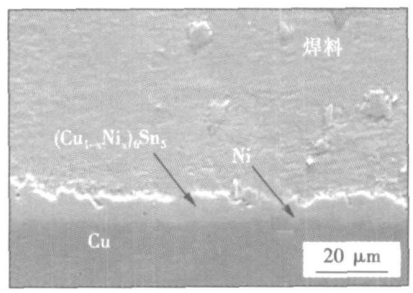

(a) SAC0307/Ni

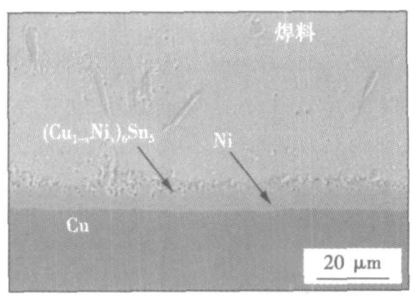

(b) SAC0307-0.05Ni/Ni

图 2 180 ℃下老化 384 h 后的界面 IMC 的形貌

Fig. 2 Morphology of IMC after aging at 180 ℃ for 384 hours

图 3 为老化时间对界面 IMC 厚度的影响. IMC 的厚度用 CAD 软件测量多次并取平均值获得. SAC0307/Ni 和 SAC0307-0.05Ni/Ni 的界面 IMC 厚度均随老化时间的增加而增加，且图中 IMC 的厚度与老化时间的平方根近似成线性关系. 这很清楚地说明了在该两种焊点体系中，IMC 层厚度都遵循抛物线生长机制，即镍焊盘界面的两种焊点体系的 IMC 生长同样满足扩散控制机制，IMC 的生长速率计算公式为

$$X - X_0 = \sqrt{Dt} \tag{1}$$

式中：X 为老化时间的界面金属间化合物厚度；X_0

为回流焊后的界面金属间化合物厚度；t 为老化保温时间；D 为金属间化合物生长速率常数. 因此，由公式可以计算出在 180 ℃下 SAC0307/Ni 和 SAC0307-0.05Ni/Ni 的界面金属间化合物生长速率分别为 1.54×10^{-5} μm²/s 和 0.46×10^{-5} μm²/s，即 SAC0307-0.05Ni/Ni 的 IMC 的生长速率明显比 SAC0307/Ni 的 IMC 生长速率小. 一是由于 SAC0307-0.05Ni/Ni 的 $(Cu_{1-x}Ni_x)_6Sn_5$ 中的 Ni 原子含量较高，老化过程中 IMC 层生长缓慢. 二是由于 SAC0307 钎料的 IMC 两侧 Ni 原子的浓度差较大，180 ℃高温长时间老化给其提供较大的扩散能，促进了 IMC 长大. 而 SAC0307-0.05Ni 钎料的 IMC 的两侧由于镍的加入降低其浓度差，从而降低了 Ni 原子的扩散速率，控制了 IMC 长大. 因此，钎料中添加 0.05% Ni（质量分数）后，焊盘镍镀层消耗比较小，表现为界面 IMC 的厚度相对较薄，靠近母材的金属间化合物面比较平整.

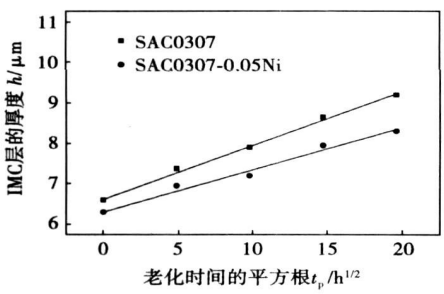

图 3　老化时间对界面 IMC 层厚度的影响

Fig. 3　Effect of aging on thickness of IMC

2.2　SAC0307-xNi/Ni 的镍焊盘消耗及 IMC 化学组成的变化

图 4 为老化时间对 SAC0307-0.05Ni/Ni 和 SAC0307/Ni 的焊盘镍层剩余厚度的影响. 做从基板经界面到钎料基体的线扫描，从而确定焊盘镍层的厚度变化规律及化合物 $(Cu_{1-x}Ni_x)_6Sn_5$ 中 Ni 原子含量的变化规律. 镍含量陡升到陡降的距离即焊盘镍层的剩余厚度. 镍陡降后含量趋于稳定的一段距离为 IMC 层厚度. 根据回流焊后和老化不同时间后的镍层厚度的线扫描曲线，利用 CAD 软件多次测量厚度值，取平均值即可得到两种焊点体系的焊盘镍层剩余厚度.

由焊盘镍层剩余厚度平均值拟合出如图 4 中曲线. 由图可知，SAC0307/Ni 和 SAC0307-0.05Ni/Ni 两种焊点体系回流焊后的镍层消耗厚度几乎相同，约为 6.21，6.57 μm. 老化 24 h 后，其厚度值约为 5.82，

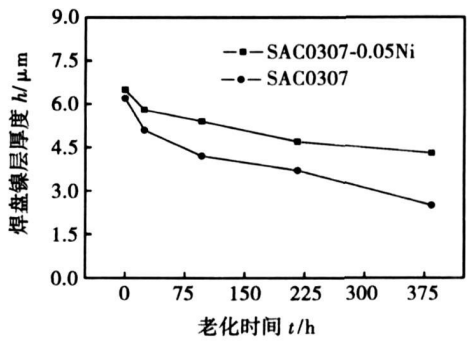

图 4　老化时间对焊盘镍层剩余厚度的影响

Fig. 4　Effect of aging on residual thickness of Ni layer

5.13 μm，SAC0307/Ni 的镍层厚度显著降低. 老化 384 h 后，镍层剩余厚度值约为 2.32，4.49 μm.

SAC0307/Ni 焊点中镍层的剩余厚度值已明显小于 SAC0307-0.05Ni/Ni 焊点的镍层剩余厚度. 钎料中添加 0.05% Ni（质量分数）后，大大降低了 SAC0307/Ni 焊点金属间化合物两侧的浓度差，高温老化过程中，在获得相同的扩散能的前提下，界面反应速率变小，减轻了镍焊盘的消耗程度，表现为镍层的剩余厚度更大. 因此，钎料中添加适量的 Ni 元素可以有效地降低焊盘镍层在老化过程中的消耗速率，即显著提高了镍焊盘的抗老化能力.

在进行分析确定化合物的组成时，由于 (Ni+Cu) 与 Sn 的原子比为 6∶5，所以生成的 IMC 相为 $(Cu_{1-x}Ni_x)_6Sn_5$，$(Cu_{1-x}Ni_x)_6Sn_5$ 相极其稳定，由于镍和铜有相似的晶格点阵，部分 Ni 原子取代 Cu 原子使其更加稳定. 有报道称在 240 ℃时 IMC 中含有 0～25%Ni（摩尔分数）. Ni 和 Cu 原子在 180 ℃老化时的互扩散不可避免，这就导致虽然化合物的类型没有改变，但是化学组成发生变化. 随着老化时间的增加，SAC0307/Ni 和 SAC0307-0.05Ni/Ni 的 IMC 中镍的含量逐渐增加. 180 ℃老化 384 h 后，SAC0307/Ni 的 IMC 中的镍含量约为 20%～21%Ni（摩尔分数），SAC0307-0.05Ni/Ni 达到约 27%～28%Ni（摩尔分数）. 由于老化过程中，镍焊盘中的 Ni 原子要扩散进入 $(Cu_{1-x}Ni_x)_6Sn_5$ 中，从而确保化合物的长大，最终导致 $(Cu_{1-x}Ni_x)_6Sn_5$ 中镍的含量随老化时间增加而增加.

3　结　　论

（1）SAC0307/Ni 和 SAC0307-0.05Ni/Ni 生成的 IMC 均为 $(Cu_{1-x}Ni_x)_6Sn_5$，随老化时间增加，IMC 的类型没有变化，但化学组成有所改变. $(Cu_{1-x}Ni_x)_6Sn_5$

化合物中镍的含量均随老化时间的增加而增加.

(2) SAC0307/Ni 和 SAC0307-0.05Ni/Ni 焊点界面的 IMC 厚度均与老化时间的平方根近似成线性关系. SAC0307-0.05Ni/Ni 比 SAC0307 焊点的 IMC 厚度小, 老化过程中的生长速率降低. 钎料中添加 0.05%Ni(质量分数)可以有效地抑制回流后和老化过程中 IMC 的生成和长大.

(3) 回流焊后, SAC0307/Ni 的焊盘剩余镍层厚度与 SAC0307-0.05Ni/Ni 的相近. 经过 180 ℃老化 384 h 后, SAC0307/Ni 的焊盘剩余镍层厚度明显比 SAC0307-0.05Ni/Ni 的小. 钎料中加入 0.05%Ni(质量分数)后显著降低了焊盘镍层在老化过程中的消耗速度即显著提高了镍焊盘的抗老化能力.

参考文献:

[1] 唐兴勇, 王 裙, 谷 博, 等. 老化对 Sn-Ag-Cu 焊料/Ni-P 镀层界面结构和剪切强度的影响[J]. 金属学报, 2006, 42(2): 205—210.
Tang Xingyong, Wang Jun, Gu Bo, *et al*. Effects of aging on structuers and shear strength of interface of Sn-Ag-Cu solder/Ni-P plating layer[J]. Acta Metallurgica Sinica, 2006, 42(2): 205—210.

[2] Pang J H L, Low T H, Xiong B S, *et al*. Thermal cycling aging effects on SnAgCu solder joint microstructure, IMC and strength[J]. Thin Solid Films, 2004, 462(7): 370—375.

[3] Kim K S, Yu C H, Yang J M. Aging treatment characteristics of solder bump joint for high reliability optical module[J]. Thin Solid Films, 2004, 462(7): 402—407.

[4] 李晓延, 杨晓华, 兑卫真, 等. 时效对 Sn-3.8Ag-0.7Cu/Cu 焊料接头的组织和拉伸性能的影响[J]. 机械强度, 2008, 30(1): 24—28.
Li Xiaoyan, Yang Xiaohua, Dui Weizhen, *et al*. Effect of aging on microstructure and tensile properties of Sn-3.8Ag-0.7Cu/Cu solder joint[J]. Journal of Mechanical Strength, 2008, 30(1): 24—28.

[5] 卢 斌, 栗 慧, 王娟辉, 等. 稀土 Er 对 Sn-3.0Ag-0.5Cu 无铅焊料合金组织与性能的影响[J]. 中国有色金属学报, 2007, 17(4): 518—524.
Lu Bin, Li Hui, Wang Juanhui, *et al*. Effect of Er on microstructure and properties of Sn-3.0Ag-0.5Cu lead-free solder alloy[J]. The Chinese Journal of Nonferrous Metals, 2007, 17(4): 518—524.

[6] Guo F, Choi S, Subramanian K N, *et al*. Evaluation of creep behavior of near-eutectic Sn-Ag solders containing small amount of alloy additions[J]. Mater Science Engineering A, 2003, 35(1): 190—199.

[7] 史耀武, 夏志东, 雷永平, 等. 电子组装生产的无铅技术与发展趋势[J]. 电子工艺技术, 2005, 26(1): 6—9.
Shi Yaowu, Xia Zhidong, Lei Yongping, *et al*. Development and trend of lead-free technology for electronic assembly manufacturing[J]. Electronics Process Technology, 2005, 26(1): 6—9.

作者简介: 王玲玲, 女, 1984 年出生, 硕士研究生. 主要从事微电子封装技术研究. 发表论文 1 篇.

Email: jolly24@163.com

[上接第 52 页]

[2] Lu S P, Fujii H, Sugiyama H, *et al*. Effects of oxygen additions to argon shielding gas on GTA weld shape[J]. ISIJ International, 2003, 43(10): 1590—1595.

[3] Lu S P, Fujii H, Nogi K, *et al*. Effect of oxygen content in He-O_2 shielding gas on weld shape in ultra deep penetration TIG[J]. Science and Technology of Welding and Joining, 2007, 12(8): 689—695.

[4] 董文超, 陆善平, 李殿中, 等. 微量活性组元氧对焊接熔池 Marangoni 对流和熔池形貌影响的数值模拟[J]. 金属学报, 2008, 42(2): 249—256.
Dong Wenchao, Lu Shanping, Li Dianzhong, *et al*. Numerical simulation of effects of the minor active-element oxygen on the Marangoni convection and the weld shape[J]. Acta Metallurgica Sinica, 2008, 44(2): 249—256.

[5] Lu S P, Dong W C, Li D Z, *et al*. Numerical study and comparisons of gas tungsten arc properties between argon and nitrogen[J]. Computational Materials Science, 2009, 45(2): 327—335.

[6] McKelliget J, Szekely J. Heat transfer and fluid flow in the welding arc[J]. Metallurgical and Materials Transactions A, 1986, 17(7): 1139—1148.

[7] Sahoo P, DebRoy T, McNallan M J. Surface tension of binary metal-surface active solute systems under conditions relevant to welding metallurgy[J]. Metallurgical Transactions B, 1988, 19B(2): 483—490.

[8] Boulos M I, Fauchais P, Pfender E. Thermal plasmas-fundamentals and applications[M]. New York: Plenum, 1994.

[9] Evans D L, Tankin R S. Measurement of emission and absorption of radiation by an argon plasma[J]. Physics of Fluids, 1967, 10(6): 1137—1144.

[10] Cram L E. Statistical evaluation of radiative power losses from thermal plasmas due to spectral lines[J]. Journal of Physics D: Applied Physics, 1985, 18(3): 401—412.

作者简介: 董文超, 男, 1979 年出生, 博士. 主要从事焊接电弧与熔池传热传质的数值模拟科研工作. 发表论文 2 篇.

Email: shplu@imr.ac.cn

metal. In addition, the welded joint by the fiber laser-MIG hybrid welding has higher Erichsen values than that by laser joints. The difference in plasticity is attributed to the microstructure changes in the welded joint of hybrid welding. Thus, the fiber laser-MIG hybrid welding of CP-Ti can be carried out successfully at higher welding speed with a good combination of weld bead appearance and plasticity.

Key words: fiber laser welding; fiber laser-MIG hybrid welding; titanium alloys; tensile test

Experimental analysis on friction hydro pillar processing of cylindrical coupling of 2024 aluminum alloy CHEN Zhonghai, CHEN Jiaqing, JIAO Xiangdong, ZHOU Canfeng (Research Centre of Offshore Engineering Joining Technology, Beijing Institute of Petrochemical Technology, Beijing 102617, China). p 37—40

Abstract: The cylindrical coupling of 2024 Aluminum alloy was welded by friction hydro pillar processing (FHPP) in the first domestic friction stitch welding machine. The diameter of the consumed metal stud is 14 mm, the depth and diameter of the predrilled hole are 25 mm and 16 mm respectively. The effects of rotational speed and shielding gas on the FHPP quality were mainly studied, and the microstructure and its properties of the sample were analyzed by means of some measuring apparatus such as optical microscope and microhardness tester etc. The results indicate that the low rotation can form the insufficient bonding, even result in the cease of the weld head motor during the welding. The quality of welded joint is better when the rotational speed is 5 000 r/min and the feeding rate is 0.5 mm/s. The shielding gas can improve the quality of FHPP with thinner fusion line, and the upper part of the metal stud is bonded to the base metal very well.

Key words: friction hydro pillar processing; friction stitch welding; 2024 aluminum alloy; microstructure; shielding gas

Experimental study on electrode wear mechanism in resistance spot welding of high strength hot galvanization steels ZHANG Xuqiang[1], ZHANG Yansong[2], CHEN Guanlong[2] (1. School of Mechanical Engineering, Petroleum University of China, Dongying 257061, Shandong, China; 2. School of Mechanical Engineering, Shanghai Jiaotong University, Shanghai 200030, China). p 41—43, 48

Abstract: Surface alloying mechanism on the electrode end face was complex and its wear was serious in welding of high strength hot galvanization steel. Elements composition and metallography experiment of the worn electrode were carried out to study the alloying on electrode end surface and microstructure evolvement. It was shown that the elements of Al, Zn etc were found in alloying layer. Different alloys were formed for different contents of Al, Zn at different temperatures, which decreased conductivity and heat conduction on electrode face. Al in coating was one of the main reasons that led to serious electrode wear. Pitting was grown obviously and micro cracks were produced at pitting region for higher temperature and pressure, the molten metal in coating penetrated into the electrode interior and accelerated electrode invalidation. The metal structure in recrystallization region was changed from columnar crystal to equiaxed crystal, which decreased hardness and anti-plastic deformation capability of electrode.

Key words: electrode wear; high strength hot galvanization steel; alloying; resistance spot welding

Oxidation of metallic particle and its effect on properties of plasma sprayed coatings WEI Qi, ZHANG Linwei, LI Hui, CUI Li (College of Materials Science and Engineering, Beijing University of Technology, Beijing 100124, China). p 44—48

Abstract: The oxidation mechanisms of iron particles and NiCoCrAlY particles during plasma spraying process and its effect on the sprayed coatings were investigated by the in-flight particles collection setup and the gas shrouding. The results show that there are two oxidation mechanisms during in-flight oxidation: one is the diffusion oxidation; the other is the convective oxidation, which are decided by the distance from the spraying particles to the nozzle. The oxidation content increases with the increasing of the standoff distance. The shrouded gas can decrease the oxidation content of in-flight particles and increase the oxidation resistance of NiCoCrAlY coatings.

Key words: plasma spraying; metallic particle; oxidation mechanism; oxidation resistance.

Numerical simulation of welding arc and surface-activating element on weld shape in TIG welding DONG Wenchao, LU Shanping, LI Dianzhong, LI Yiyi (Shenyang National Laboratory for Materials Sciences, Institute of Metal Research, Chinese Academy of Sciences, Shenyang 110016, China). p 49—52, 56

Abstract: Welding arc and weld pool models were established by FLUENT software for spot and moving TIG welding of SUS304 stainless steel to investigate the effect of the surface-activating element oxygen on the weld shape and analyze the properties of argon arc and helium arc and their effects on the weld shape. The results show that the change of the Marangoni convection induced by different oxygen contents can be considered as one of the principal factors to increase penetration. The plasma drag force from the argon arc has obvious effect on the weld shape. Compared with the argon arc, the helium arc is more constricted, the welding current density is much greater and the much more heat flux is transferred into the weld pool, which increase the inward convection induced by the electromagnetic force, thus the deeper weld depth can be obtained. The calculated weld D/W ratio agrees with that of the experiment.

Key words: weld shape; welding arc; surface-activating element; numerical simulation

IMC of SAC0307-*x*Ni/Ni soldered joint and consumption of Ni coating WANG Lingling, SUN Fenglian, WANG Lifeng, ZHAO Zhili (School of Materials Science & Engineering, Harbin University of Science and Technology, Harbin 150040, China). p 53—56

Abstract: The microstructure of interfacial IMC and the consumption of Ni layer for SAC0307/Ni (Sn-0.3Ag-0.7Cu/Ni) soldered joint and SAC0307-0.05Ni/Ni (Sn-0.3Ag-0.7Cu-0.05Ni/Ni) soldered joint after aging at 180 ℃ were studied by scanning electron microscope (SEM). The results indicated that the IMC layer of SAC0307/Ni and SAC0307-0.05Ni/Ni are both $(Cu_{1-x}Ni_x)_6Sn_5$ after reflow soldering. With the increasing of aging time, the thickness of IMC layer increases gradually, the type of IMC is not changed, but the chemical composition changes. The morphology of IMC is storm-

shaped and the thickness of IMC is much thinner when SAC0307 solder added 0.05% Ni is used. The consumption of Ni layer is nearly the same using both solders after the first time reflow soldering, but the residual thickness of the Ni layer in SAC0307/Ni solder is thinner than that in SAC0307-0.05Ni/Ni after aging for 384 h. So solders with a little Ni element can decrease the consumption rate of Ni layer effectively during aging, that is, the aging-resistant ability of Ni pad is improved obviously.

Key words: SAC0307-*x*Ni; solder; Ni substrate; IMC; aging

Wettability of molten $Zr_{55}Al_{10}Ni_5Cu_{30}$ metallic glass brazing alloy on α-Al_2O_3 and ZrO_2 ZHENG Xiaohong, SHEN Ping (Key Laboratory of Automobile Materials Ministry of Education, Jilin University, Changchun 130025, China). p 57—60, 64

Abstract: The wettability and interfacial characteristics of molten $Zr_{55}Al_{10}Ni_5Cu_{30}$ metallic glass brazing alloy on polycrystalline α-Al_2O_3 and ZrO_2 substrates were studied using a modified sessile drop method. The results show that the wettability of the $Zr_{55}Al_{10}Ni_5Cu_{30}$/$\alpha$-$Al_2O_3$ system is excellent with the final contact angles approaching zero degree at 1 133-1 193 K. However, the wettability of the $Zr_{55}Al_{10}Ni_5Cu_{30}$/$ZrO_2$ system is poor, but it can be progressively improved with the elapse of time during the isothermal dwelling in the temperature range of 1 133-1 253 K. A certain extent of interfacial reaction happens in both systems. The investigation on the spreading kinetics and interfacial microstructure indicates that the adsorption of the active atoms such as Zr at the interface, particularly at the triple junctions, plays a key role in determining the wettability, whereas the contribution of the interfacial reaction is relatively minor.

Key words: Metallic glass brazing alloy; wettability; interfacial reaction; adsorption

Microstructure and mechanical properties of magnesium alloy AZ31B joint brazed with Al-Mg-Zn filler metal MA Li[1], HE Dingyong[1], LI Xiaoyan[1], JIANG Jianmin[1], WANG Lizhi[2] (1. College of Materials Science and Engineering, Beijing University of Technology, Beijing 100124, China; 2. Welding Research Institute of Central Research Institute of Building & Construction, China Metallurgical Group Corporation, Beijing 100088, China). p 61—64

Abstract: High-frequency induction brazing of wrought magnesium alloy AZ31B with Al-Mg-Zn filler metal was investigated. Microscopic structure, the phases and the mechanical properties of brazed joint were studied. The microstructure and formation phases at the interface in the brazed joint were investigated by scanning electron microscopy (SEM), X-ray diffraction instrument (XRD) and energy dispersive spectrometer (EDS). The strength of the brazed joint and the microhardness of the formation phases were also tested. The results show that, Al-Mg-Zn filler metal reacting with the base metal AZ31B, and α-Mg+β-$Mg_{17}(Al, Zn)_{12}$ divorced eutectic structure is formed in the brazed joint. Microhardness of the base metal AZ31B is the smallest and β-$Mg_{17}(Al, Zn)_{12}$ phase of the brazed joint is the hardest. Both the butt joint and the overlap joint exhibit intergranular fracture mode, the fracture comes from hard brittle phase β-$Mg_{17}(Al, Zn)_{12}$ of α-Mg+β-Mg17$(Al, Zn)_{12}$ divorced eutectic structure.

Key words: AZ31B magnesium alloy; Al-Mg-Zn filler metal; brazing; divorced eutectic; joint strength

Failure of soldered joint during thermal fatigue test LIN Jian[1], LEI Yongping[1], ZHAO Haiyan[2], WU Zhongwei[1] (1. College of Materials Science and Engineering, Beijing University of Technology, Beijing 100124, China; 2. Department of Mechanical Engineering, Tsinghua University, Beijing 100084, China). p 65—68, 72

Abstract: The failure process of soldered joint in SMT was investigated by electrical resistance measurement method and crack observation method. The characteristics of electrical resistance value variation of lead-tin and lead-free soldered (SAC305) joints during the thermal fatigue test were obtained. And at the same time the crack propagation in soldered joint was observed. According to these measurements, the failure rules of lead-tin and lead-free soldered joint were compared. The relationship between electrical resistance value variation and crack propagation of soldered joint during thermal fatigue test was studied by FEM, and an empirical criterion to estimate the failure of the soldered joint in the thermal fatigue test was obtained based on electrical resistance value variation. The experimental results show that the lead-free soldered joint has a higher resistibility in thermal fatigue than the traditional lead-tin soldered joint. The criterion based on electrical resistance value variation was founded from the experimental and simulation results.

Key words: SMT; soldered joint; thermal fatigue; electrical resistance; crack

TiN/Ti composite coating deposited on titanium alloy substrate by reactive electric-spark HAO Jianjun[1,2], PENG Haibin[1], HUANG Jihua[3], MA Yuejin[1], LI Jianchang[1] (1. College of Electromechanical Engineering, Agriculture University of Hebei, Baoding 071001, Hebei, China; 2. Light Metal Materials Engineering Research Center of Hebei, Baoding 071000, Hebei, China; 3. School of Materials Science and Engineering, University of Science and Technology of Beijing, Beijing 100083, China). p 69—72

Abstract: TiN/Ti composite coating was deposited on TC4 titanium alloy substrate with the self-made special gas-filled-closed electric-spark deposition device and electric-spark deposition machine modeled DZ-1400, the industry pure titanium (TA2) was used as electrode and the industry pure nitrogen gas as shielding and reacting atmosphere. The microstructures, interfacial behavior, phase and element in the coatings were investigated by scanning electronic microscope, X-ray diffraction and X-ray photo spectrum. The microhardness of coatings was tested and its wear-resistance property was tested by the self-made abrasion machine and compared with W18Cr4V rapid steel treated by quenching. The results show that an excellent bonding between the coating and substrate is ensured by the strong metallurgical interface. The coatings are mainly composed of Ti and synthesized TiN. The highest microhardness of coating reaches to 1 388 HV0.1, which is six times higher than that of the substrates. Wear resistance of the coatings is excellent.

Key words: reactive electric-spark deposition; TiN; composite coating; titanium alloy

Influence of transverse alternative magnetic field frequency on microstructure and properties of plasma arc surfacing layer LIU Zhengjun, ZHAO Qian, CI Honggang, SU Yunhai (School of